Pol. J. Environ. Stud. Vol. 34, No. 4 (2025), 4393-4407
DOI: *10.15244/pjoes/190006* ONLINE PUBLICATION DATE: 2024-09-16

Original Research

The Spatiotemporal Relationship of LUCE and ESV Based upon a Grid Square – A Case Study of Anhui Province, China

Kun Zhang[1, 2]*, Xinghui Zhang[1, 2], Liang-ji Xu[1, 2], Xiaopeng Liu[1, 2], Yanhai Zhang[3]

[1]State Key Laboratory of Mining Response and Disaster Prevention and Control in Deep Coal Mines, No. 168 Taifeng Street, Huainan, China
[2]School of Spatial Informatics and Geomatics Engineering, Anhui University of Science and Technology, No. 168 Taifeng Street, Huainan, China
[3]Huaibei Mining (Group) Co., Ltd., No. 276, Renmin Middle Road, Huaibei, China

Received: 13 April 2024
Accepted: 12 June 2024

Abstract

Amid the dual objectives of "low carbon" and "ecological environmental protection", focusing on Anhui Province, this study examined the spatial and temporal dynamics of land use carbon emissions (LUCE) and ecosystem service value (ESV) using grid analysis and models like GM and PLUS. The study highlights the substantial expansion of construction land from 2000 to 2020, witnessing a growth of 4726.92 km^2, primarily attributed to cultivated land, comprising 98.34% of the increase. Net carbon emissions exhibited an inverted "V"-shaped growth trend, surging by 10228.30×10^4 tons. The ESV in Anhui Province showed an "M"-shaped slow growth trend, with an increase of 1.14%. The difference in ESV intensity between north and south is obvious, and the southern part of Anhui province as a whole is the northern part. A substantial spatial negative correlation exists between ESV intensity and carbon emission intensity and obvious aggregation characteristics. The industrial resource-oriented cities of Huaibei, Maanshan, Huainan, and Anqing emerge as the primary carbon sources, contributing 60.72% to 71.98% of the total carbon emissions in Anhui Province. These findings offer valuable insights for Anhui Province to devise rational land use policies toward achieving low-carbon green development goals.

Keywords: carbon emission, GM-PLUS model, ecosystem service value, spatial autocorrelation, land use

Introduction

In the context of global warming, carbon emissions have garnered escalating global attention [1, 2]. Controlling carbon emissions and mitigating climate change represents a shared mission for all nations. In pursuit of this goal, China has implemented the Double-Carbon target, with objectives to peak carbon emissions by 2030 and attain carbon neutrality by 2060 [3].

In the process of industrialization and urbanization, a large amount of fossil fuels were consumed, resulting

*e-mail: chzk@aust.edu.cn;
Tel.: +8-613-540-598-446.

in significant carbon emissions, and alterations occurred in land use types [4]. There exists a complex relationship between land use change and carbon emissions [5, 6]. Moreover, land use change significantly impacts ecosystems by reshaping the spatial distribution of regional biodiversity, resources, and ecosystem types. This alteration can influence ecosystem services, which can often be evaluated in economic terms, such as through Ecosystem Service Value (ESV) [7, 8]. Therefore, variations in carbon emissions and ESV, along with their spatiotemporal relationship, can be analyzed based on land use change, an endeavor of paramount importance for mitigating carbon emissions, enhancing the ecological environment, and fostering sustainable development.

In recent years, research has delved into the ramifications of land use change on carbon emissions and ESV, such as spatial differences in carbon emissions at various regional scales [9, 10], carbon emission mechanisms of single land types [11, 12], the relationship between land use change and carbon sources and sinks [13, 14], and spatiotemporal characteristics and interrelationships between ESV and land use change [15, 16]. Wei Wei and Yahui Zhang et al. explored the temporal and spatial evolution characteristics of LUCE at provincial and county scales, respectively [17, 18]. Luo Xiang et al. used the DEA and SBM-undesirable models to determine the constraint benefits of cultivated land carbon emissions on land use efficiency [11]. Wang Fu et al. studied the temporal and spatial changes of land use change on carbon sources and carbon sinks under different climate conditions and found that climate and land use change are the main reasons affecting carbon sinks [14]. Guo Pengfei et al. explored the impact of land use change on ESV from the spatial dimension and revealed the response mechanism of ESV [19]. However, there is a scarcity of studies investigating the spatiotemporal correlation between carbon emissions and ESV derived from grid scale land use changes.

An integral part of the Yangtze River Delta Economic Circle, Anhui Province in East China boasts the highest urbanization rate, densest urban clusters, and top economic development nationwide [20]. Anhui Province is also an important coal base, ensuring the energy demand for economic development in East China [21]. The fluctuations in carbon emissions and ESV within Anhui Province correlate with the sustainable development of China's eastern region. Therefore, this study aims to investigate the spatiotemporal relationship between carbon emissions and ESV in Anhui Province and analyze their spatial correlation.

Material and Methods

Study Area

Situated in eastern China, Anhui Province, with its capital Hefei, comprises 16 prefecture-level cities, covering an area of 14.01×10^4 km^2 (Fig. 1). Positioned in the lower reaches of the Yangtze River and Huai River, Anhui serves as a transitional zone between warm temperate and subtropical climates. The landform consists of plains, hills, and mountains. The northern part of Anhui is the Huaibei Plain, which is a grain producing area rich in crops such as wheat and corn. It is also an important coal producing base where the famous Huainan and Huaibei mining areas are located. The central part is the Jianghuai Hills and the plain along the Yangtze River, with rice as the main crop. It is an important industrial area, with 8 out of 10 cities with a high level of industrialization in the province located here. The southern region is mountainous, with agriculture and tourism as the main industries. In 2022, the permanent population of the region stood at 61.27 million, accompanied by a GDP of approximately 643.5 billion US dollars.

Materials

The land use data is sourced from the Wuhan University CLCD dataset [22], which is suitable for long time series land use change studies with high temporal resolution and accuracy validation up to 80%. According to the land use classification criteria of the

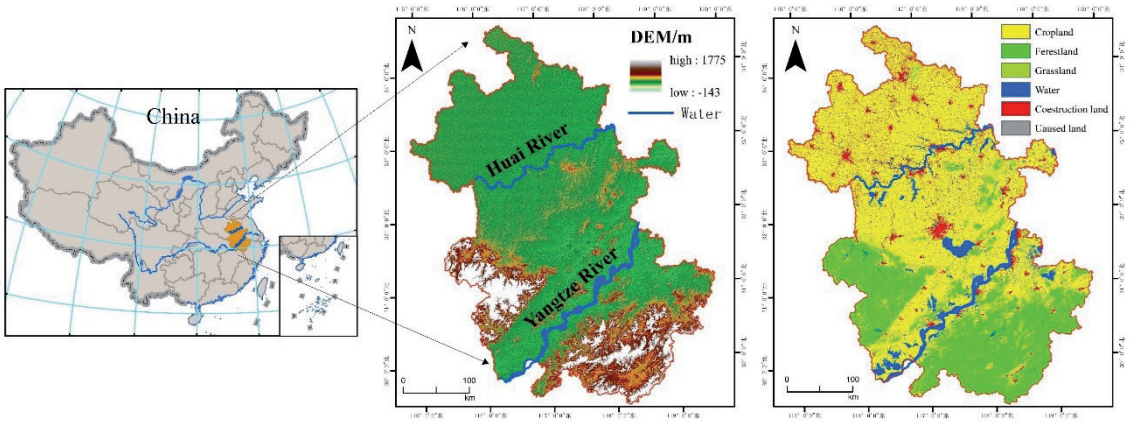

Fig. 1. The geographical location of the study area.

Table 1. Data details.

Datasets	Data	Year	Attributes / Spatial Resolution	Data Resources
Land-use datasets	Land-use data	2000, 2005, 2010, 2015, 2020	TIFF/30 m	https://zenodo.org/records/
Vector datasets	Administrative boundaries	2022	SHP	National Catalogue Service for Geographic Information (https://www.webmap.cn/)
	Road network data	2020		
	River network data	2022		
Physical geographical data	DEM	2020	TIFF/30 m	Resource and Environmental Science Data Platform (https://www.resdc.cn/Default.aspx)
	Average annual precipitation	2015	TIFF/1 km	
	Average annual temperature	2015		
Socioeconomic data	GDP	2020		
	Population	2020		
Statistic data	Energy consumption data	2000-2022	Excel	Anhui Municipal Statistical Yearbook, China Energy Statistical Yearbook
	GDP			
	Population			

Chinese Academy of Sciences, the land classes in the CLCD dataset are divided into six first-level land classes, namely, cropland, forestland, grassland, water, construction land, and unused land. Socio-economic data for Anhui Province and energy consumption data primarily come from the Anhui Municipal Statistical Yearbook and China Energy Statistical Yearbook. Vector data from the National Catalogue Service for Geographic Information, including roads, rivers, and administrative boundaries, predominantly originate (Table 1). Anhui Province underwent administrative division adjustments from 2000 to 2015, dividing Chaohu Lake into Hefei, Wuhu, and Ma'anshan, and dividing Shouxian County from Lu'an City to Huainan City. The technical route is shown in Fig. 2.

Research Methods

Carbon Emissions Estimation

Land use carbon emissions (LUCE) include those from non-construction land as well as from construction

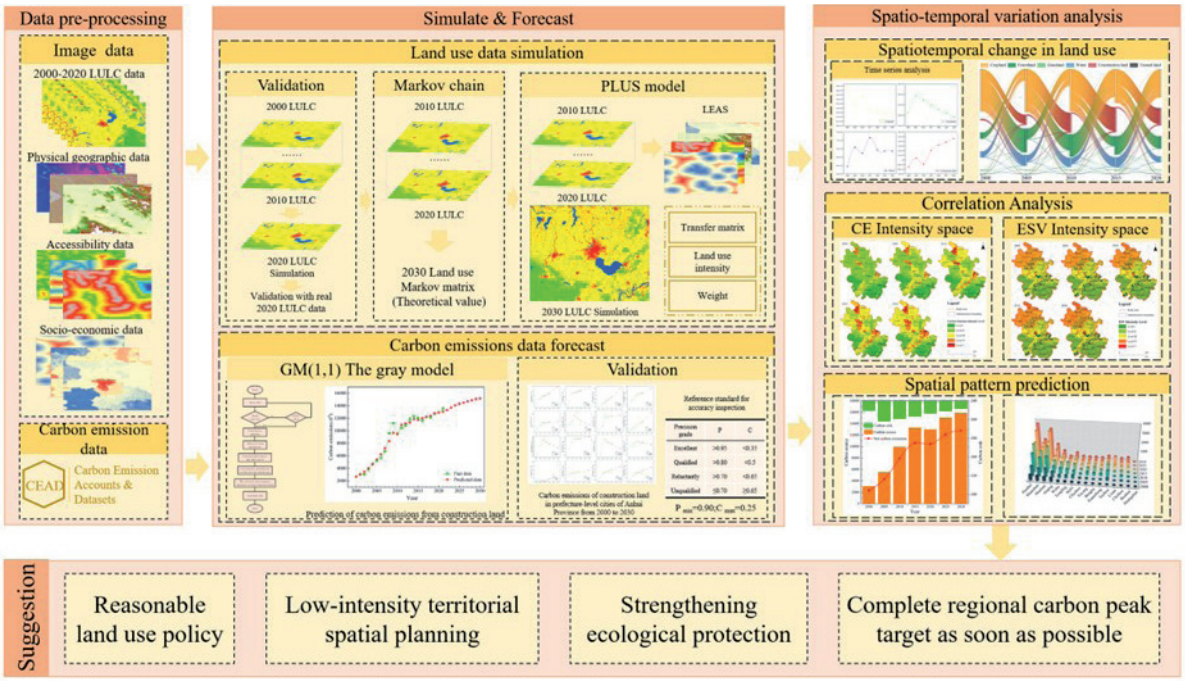

Fig. 2. Study framework.

land [23]. Carbon emissions from non-construction land can be estimated directly by multiplying the area of each land use type and the corresponding carbon emission factor and then summing them up. Estimating carbon emissions from construction land involves an indirect approach based on fossil energy consumption data for calculation [24].

The equation for estimating carbon emissions from non-construction land can be expressed as follows:

$$E_1 = \sum S_i \times G_i \tag{1}$$

Style: E_1 is carbon emissions from non-construction land: S_i is the area of land type *i;* G_i is the carbon sink or emission factor for land type *i*.

The carbon emission coefficient for each land use type was established by consulting pertinent literature and considering the specific conditions of the study area [23, 25], as illustrated in Table 2.

To estimate carbon emissions from construction land, this text uses consumption data and carbon emission coefficients obtained from various sources (Table 3), including the China Energy Statistical Yearbook, the Anhui Statistical Yearbook, and the Intergovernmental Panel on Climate Change (IPCC). The equation can be expressed as follows:

$$E_2 = \sum_{i=1}^{8} (T_i \times \theta_i \times \varphi_i) \tag{2}$$

Style: E_2 is direct carbon emissions, T_i is the average annual consumption of each type of fossil energy source, θ_i is all kinds of fossil energy conversion standard coal coefficient, φ_i is the energy carbon emission coefficient.

The determination of land use carbon emission intensity relied on the area and carbon emission coefficient of each land type within the grid. It represents the carbon emissions per unit grid area, with higher intensity indicating greater ecological risk. The unit grid size in this paper is 2×2 km.

$$C = \sum_{i=1}^{n} \frac{S_i \times \omega_i}{S} \tag{3}$$

Style: C is the carbon emission intensity of land use, S_i is the area of the i land use type in the grid, ω_i is the carbon emission factor for the i land type, and S is the grid area.

Table 3. Various energy standard coal and carbon emission conversion coefficient.

Type	Standard coal conversion coefficient	Carbon emission coefficient
Coal	0.7143	0.7559
Cleaned coal	0.9000	0.7559
Coke	0.9714	0.8550
Natural gas	1.3301	0.4483
Kerosene	1.4714	0.5714
Diesel	1.4571	0.5921
Crude oil	1.4286	0.5857
Gasoline	1.4714	0.5538
Fuel oil	1.4286	0.6185
Electricity	0.4040	0.7935

ESV Estimation

ESV was determined using the equivalent factor method, referencing the "ecosystem service value equivalent per unit area scale" proposed in the relevant literature. One ESV equivalent was defined as 1/7 of the average annual natural food production per hectare of farmland [26]. Utilizing data on the sowing areas, yields, and prices of the three main crops of rice, wheat, and corn in Anhui Province from 2000 to 2020, the ESV unit equivalent in Anhui Province was calculated to be 1537.78 CNY/hm^2. The equation can be expressed as follows:

$$E_a = \frac{1}{7} \sum_{i=1}^{n} \frac{m_i p_i q_i}{M} \tag{4}$$

Style: E_a is the unit equivalent of ESV (CNY/hm^2); m_i is the area under crop i (hm^2); p_i is the average price of crop i in Anhui Province from 2000 to 2020 (CNY/t); q_i is the crop i yield per unit area (t/ hm^2); M is the total area under crop cultivation (hm^2).

Due to the differences in ecosystems in different geographical areas, the ESV coefficients for each category in the study area need to be corrected. The ESV table was revised based on the ratio of grain production in the research area to national grain production [27]. The correction results are shown in Table 4. In this case, the ESV of the construction land is taken as 0 [15].

Table 2. Carbon emissions coefficients of land use type. (carbon sink is negative and carbon emissions are positive).

Types	Cropland	Forestland	Grassland	Water	Unused land
Carbon emission factor (t/hm^2))	0.422	-0.644	-0.021	-0.253	-0.005

ESV:

$$V_{ESj} = \sum_{i=1}^{n} A_{ij} \times C_i \quad (5)$$

$$V_{ES} = \sum_{j=1}^{m} V_{ESj} \quad (6)$$

ESV intensity:

$$\bar{V}_{ESj} = \sum_{i=1}^{n} \frac{V_{ESj}}{S} \quad (7)$$

Style: V_{ESj} is the ESV of land types *j*, A_{ij} is the area of land use types *i* in grid *j*, C_i is the ESV factor for land types *i*; *S* is the grid area; n for 6 land use types, m is the number of grids.

Bivariate Spatial Autocorrelation Analysis

The spatial correlation and degree of aggregation between carbon emission intensity and ESV intensity in Anhui Province were analyzed using the Bivariate Moran's I method.

$$I = \frac{\sum_{i=1}^{n} \sum_{j=1}^{n} w_{ij} (x_i - \bar{x}) (x_j - \bar{x})}{S^2 \sum_{i=1}^{n} \sum_{j=1}^{n} w_{ij}} \quad (8)$$

$$I_i = \frac{(x_i - \bar{x}) \sum_{j=1}^{n} w_{ij} (x_i - \bar{x})}{S^2} \quad (9)$$

Style: *I* and I_i are global and local bivariate variables for carbon emission intensity and ESV intensity, respectively Moran's; *n* is the grids number; w_{ij} is the n × n spatial weight matrix; x_i and x_j are the attribute values of grids *i* and *j,* respectively; $\bar{x}$ and S^2 are the mean and variance of the attribute values.

Carbon Emission Prediction

Predictions for LUCE encompass forecasts for both construction and non-construction land. The carbon emissions from construction land were directly predicted using the gray GM(1,1) model [10, 28, 29]. For non-construction land, the PLUS model was utilized to predict spatial distribution, which was then combined with carbon emission coefficients to estimate emissions [30].

Table 5. Gray model prediction accuracy standard.

Accuracy Class	Excellent	Qualified	Unqualified	Poor
P	>0.95	>0.80	>0.70	≤0.70
C	<0.35	<0.50	<0.65	≥0.65

Based on the carbon emission data from construction land in prefecture-level cities of Anhui Province spanning 2000 to 2020, a first-order linear differential equation was formulated utilizing the GM(1,1) gray model to forecast carbon emissions from construction land from 2020 to 2030 [29]. Comparing the selected prediction results from 2010 to 2020 with the original data validates the accuracy of the predictions (Table 5). The maximum value of the posteriori difference ratio "*C*" is 0.25, and the minimum value of the probability of small error "*P*" is 0.90, indicating satisfactory model performance.

Employing the PLUS model, the spatial distribution of land use in 2020 and 2030 was projected based on data spanning from 2000 to 2020 in Anhui Province. The comparison between selected land use prediction outcomes for 2020 and the original data validated the accuracy of the predictions, yielding a Kappa value of 0.84, signifying excellent model performance. By leveraging the outcomes of land use prediction and carbon emission coefficients from non-construction land, carbon emissions from Anhui Province for the period of 2020-2030 were estimated.

Results

Temporal and Spatial Changes in Land Use

Table 6 and Fig. 3 illustrate, from 2000-2020, the intricate transfer changes among various land use types in Anhui Province. The total transfer area amounts to 11,374.77 km^2, representing 8.12% of the Anhui Province. The primary land types undergoing transfer and alteration are cropland and construction land. Cropland contributed the most to the transferred area, with 8103.52 km^2 transfer-out and 2791.45 km^2 transfer-in, for a total reduction of 5312.07 km^2. The transfer of cropland to construction land encompassed 4,648.42 km^2, constituting 57.36% of the total transfer-out area. Additionally, 2277.62 km^2 was transferred to forestland, accounting for 28.11%

Table 4. ESV coefficients for each category in Anhui Province (CNY/hm^{-2}a^{-1}).

Types	Cropland	Forestland	Grassland	Water	Unused land
ESV factor	6074.242	30290.47	18550.78	136578.2	1691.561

Table 6. Land use transfer matrix from 2000 to 2020.

Year	Types		2020						
			Cropland	Forestland	Grassland	Water	Construction land	Unused land	Transfer-out
2000	Cropland	Area change/km^2	80561.15	2277.62	4.02	1173.26	4648.42	0.20	8103.52
		Percentage /%		28.11%	0.05%	14.48%	57.36%	0.00%	100.00%
	Forestland	Area change/km^2	1864.01	34239.22	5.04	5.09	141.32	0.14	2015.61
		Percentage /%	92.48%		0.25%	0.25%	7.01%	0.01%	100.00%
	Grassland	Area change/km^2	61.86	19.12	33.30	2.57	14.65	0.37	98.58
		Percentage /%	62.75%	19.40%		2.61%	14.86%	0.38%	100.00%
	Water	Area change/km^2	807.37	8.01	0.03	5641.14	123.64	0.20	939.25
		Percentage /%	85.96%	0.85%	0.00%		13.16%	0.02%	100.00%
	Construction land	Area change/km^2	56.61	0.18	0.01	149.18	8272.93	0.12	206.10
		Percentage /%	27.47%	0.09%	0.01%	72.38%		0.06%	100.00%
	Unused land	Area change/km^2	1.60	0.00	0.08	5.05	4.99	0.32	11.72
		Percentage /%	13.65%	0.01%	0.65%	43.11%	42.59%		100.00%
	Transfer-in	Area change/km^2	2791.45	2304.93	9.18	1335.15	4933.02	1.03	

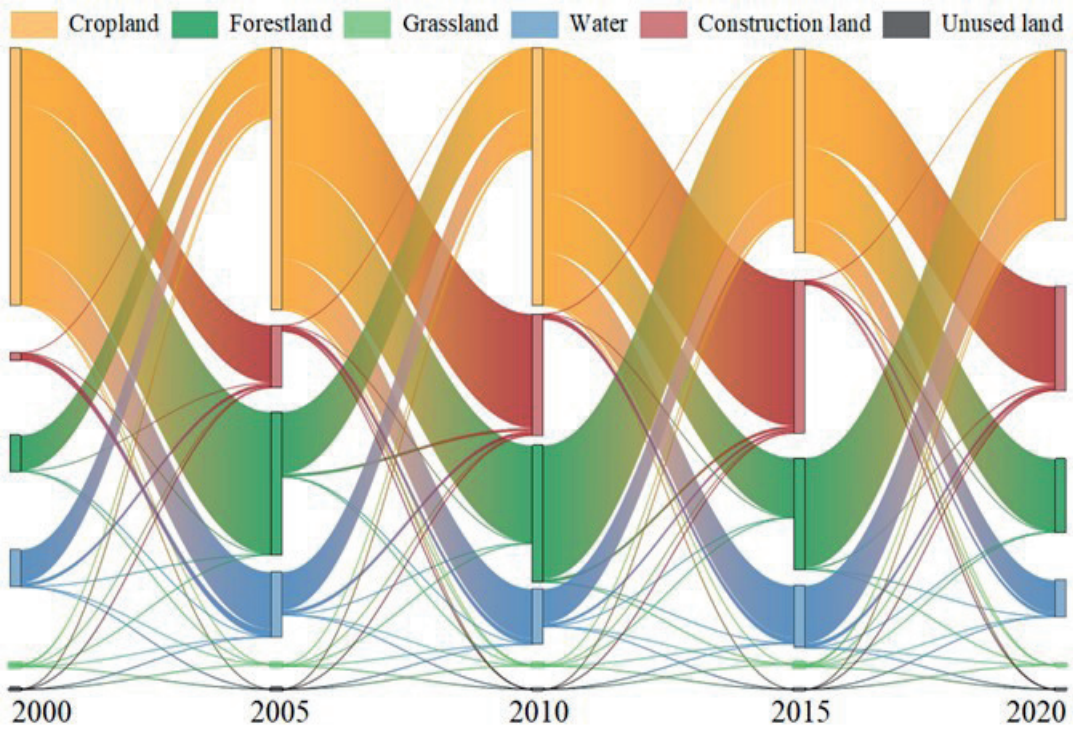

Fig. 3. Land use transfer Sankey diagram from 2000 to 2020.

Table 7. Carbon emissions of land use in Anhui Province (10^4t).

Year		2000	2005	2010	2015	2020
Carbon source	Cropland	374.16	357.59	365.26	353.33	351.75
	Construction land	2662.55	5160.81	9582.12	12918.01	12637.24
	Total	3036.72	5518.41	9947.39	13271.36	12989.00
Carbon sink	Forestland	-233.48	-243.72	-241.27	-238.10	-235.34
	Grassland	-0.03	-0.02	-0.02	-0.02	-0.01
	Water	-16.65	-17.80	-17.45	-18.39	-17.65
	Unused land	-0.01	-0.01	-0.01	-0.01	-0.01
	Total	-250.16	-261.54	-258.74	-256.50	-253.00
Net carbon emissions		2786.56	5256.87	9688.65	13014.85	12736.00

of the total transfer-in area, which promoted the expansion of forestland area. The increase of cultivated land primarily originated from forestland and water areas. Specifically, forestland accounted for 1,864.01 km^2 of transfers, comprising 66.78% of the total transferred area, while water areas contributed 807.37 km^2, representing 28.92% of the total transferred area.

The change of construction land is less than that of cultivated land, transfer-out 206.10 km^2 and transfer-in 4,933.02 km^2, with the transfer-in area significantly larger than the transfer-out area, and the total area increasing from 8,479.03 km^2 to 13,205.95km^2, with the total area showing an upward trend. From 2010 to 2015, the most notable expansion occurred in construction land encroaching on cropland, construction land increased by 1,667.25 km^2, of which 1,649.89km^2 encroached upon cropland, comprising 98.96% of the cropland transfer-out area.

Analysis of LUCE

Table 7 illustrates the stage-type growth trend of LUCE in Anhui Province from 2000 to 2020, initially rising and later declining. From 2000 to 2015, there was a substantial increase in net carbon emissions, rising from 2786.56×10^4 tons to 12736.00×10^4 tons, marking an increase of 10228.30×10^4 tons, and the average annual growth was 17.85%. The main source of carbon emissions is construction land, accounting for 87.68% to 97.34% of carbon emissions. From 2000 to 2015, as the level of urbanization increased significantly, the construction land area and energy consumption increased significantly, and net carbon emissions also increased significantly. Thereafter, due to the implementation of the "13^{th} Five-Year" energy conservation and emission reduction implementation plan of Anhui Province, coupled with the impact of the COVID-19 pandemic, which has resulted in a decline in energy consumption in 2020 [31], net carbon emissions showed a decreasing trend from 2015 to 2020. Carbon emissions from cropland showed an overall slow decline due to the reduction of cropland area, declining from 374.16×10^4 tons in 2000 to 351.75×10^4 tons in 2020, and the average annual decline was 0.30%.

The total carbon sink also tends to increase and then decrease from 2000 to 2020. Forestland is the most important carbon sink, contributing 92.83% to 93.33% of carbon sequestration, which declined after 2005. While the carbon sink of water areas fluctuates, the overall trend indicates growth.

The carbon emission intensity is categorized into five levels (I, II, III, IV, and V) based on grid carbon emissions, ranging from low to high (Fig. 4). From 2000 to 2020, there was a noticeable increase in the overall trend of carbon emission intensity in Anhui Province, and the maximum value of carbon emission intensity increased from 137.40t/hm^2 in 2000 to 450.69t/hm^2 in 2020, an increase of 2.28 times. The number of grids in classes V and IV increases by 11.60% from 2000 to 2020; the number of grids in classes I and II decreases year by year, by 44.58% in 20 years, with a clear characteristic shift towards class III.

Spatial and Temporal Variation Analysis of ESV

Table 8 illustrates an M-shaped growth trend in the overall ESV of Anhui Province from 2000 to 2020, with the overall ESV increasing from CNY 2537.95×10^8 in 2000 to CNY 2566.84×10^8 in 2020, reflecting a 1.14% increase. Forestland, water, and cropland emerged as the primary contributors to ESV in terms of each land use type, accounting for 43.27%, 36.94%, and 20.03% in that order. Among the remaining land types, the contribution of grassland declined slightly, and that of unused land remained stable. From the composition of land use, it was obtained that during the 20 years, construction land, forestland, and water areas showed different degrees of expansion, continuously encroaching on cropland, grassland, and unused land were all reduced to different degrees. However, the expansion of forestland and water area offset the construction land's encroachment on cropland, resulting in a total ESV increase of CNY 28.89×10^8.

Fig. 5 illustrates that there are obvious spatial

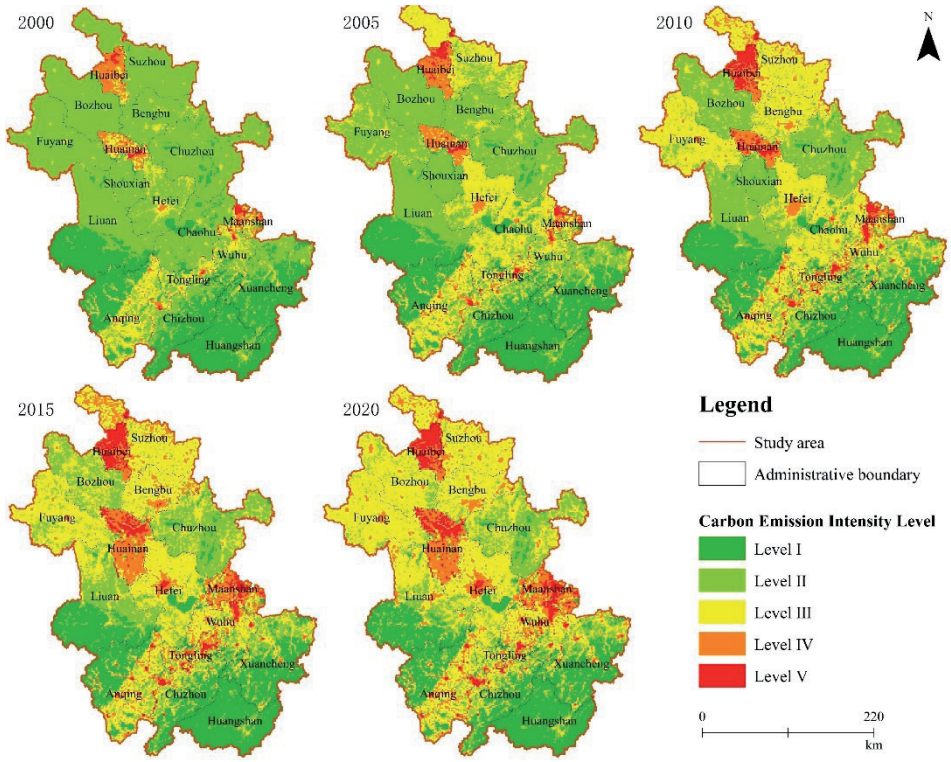

Fig. 4. Spatial patterns of carbon emission intensity on land use.

Table 8. ESV statistics of Anhui Province.

Year	Item	Cropland	Forestland	Grassland	Water	Unused land	Toal
2000	ESV/10^8	538.57	1098.18	2.45	898.74	0.02	2537.95
	ESV change rate/%	21.22%	43.27%	0.10%	35.41%	0.01%	100%
2005	ESV/10^8	514.71	1146.32	1.76	961.05	0.01	2623.85
	ESV change rate/%	19.62%	43.69%	0.07%	36.63%	0.01%	100%
2010	ESV/10^8	525.76	1134.83	1.89	941.82	0.01	2604.30
	ESV change rate/%	20.19%	43.58%	0.07%	36.16%	0.01%	100%
2015	ESV/10^8	508.58	1119.90	1.47	992.62	0.01	2622.58
	ESV change rate/%	19.39%	42.70%	0.06%	37.85%	0.01%	100%
2020	ESV/10^8	506.30	1106.94	0.79	952.81	0.01	2566.84
	ESV change rate/%	19.72%	43.12%	0.03%	37.12%	0.01%	100%

differences in ESV intensity in Anhui Province, and the overall ESV intensity in southern Anhui Province is higher than that in northern Anhui Province. Level IV ESV intensity exhibits a broad distribution range, encompassing 39.8% of total grid numbers, primarily concentrated in areas like Dabie Mountain and southern Anhui Province. Main land use types include grassland and forestland. ESV intensity in the V interval accounted for a smaller proportion, comprising only 6.04% of total grid numbers, the main land use type for the waters, mainly distributed in the Chaohu Lake and other waters. Compared with other years, there is a significant increase of 50.18% in level I grid from 2010 to 2020, and there is a phenomenon of transferring from level II to level I. Meanwhile, the level II grid is mainly distributed in Huaibei Plain, with cropland and construction land being the primary land use types.

Correlation Analyses

Table 9 reveals that the P-values of the correlation test results between ESV intensity and carbon emission intensity in Anhui Province are all below 0.001, and the global Moran's I values are all negative. This highlights a significant negative spatial correlation between carbon emission intensity and ESV intensity in Anhui Province,

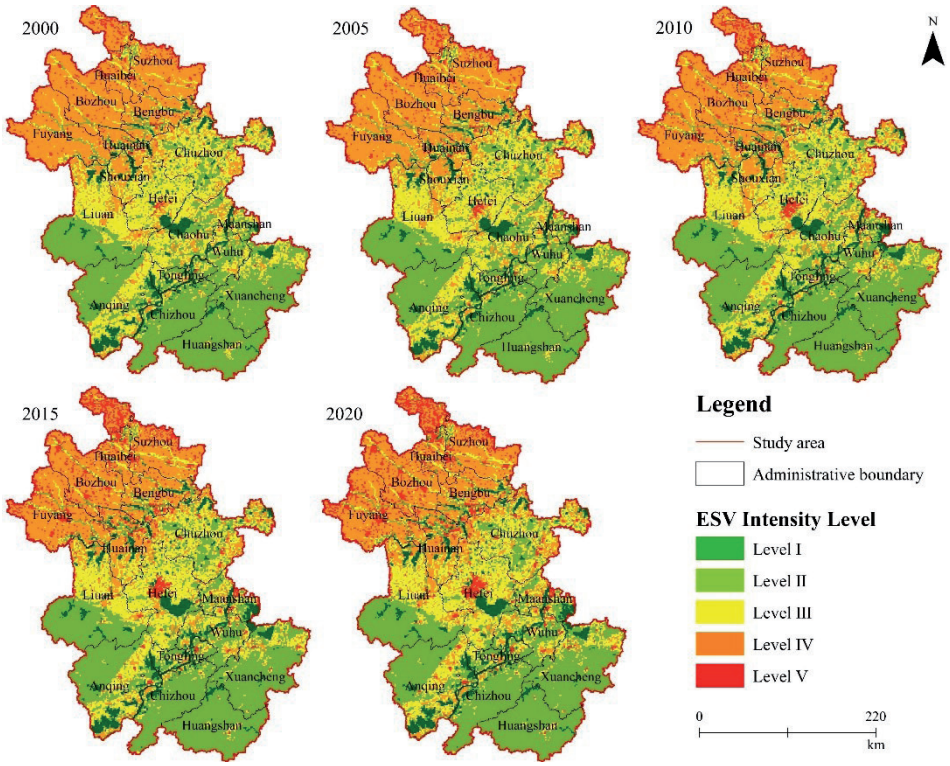

Fig. 5. Spatial distribution of ESV intensity grades in Anhui Province.

Table 9. Bivariate global Moran's I statistic.

Variate	2000	2005	2010	2015	2020
Moran's I	-0.062	-0.095	-0.100	-0.104	-0.115
P-value	<0.001	<0.001	<0.001	<0.001	<0.001
Z-value	-50.7757	-78.182	-83.569	-88.871	-97.460

where higher carbon emission intensity corresponds to lower ESV intensity. Furthermore, the decline in Moran's I suggests a spatial transition from dispersion to concentration.

Analyzing the LISA cluster graph (Fig. 6), it becomes apparent that there are distinct spatial clustering characteristics between carbon emission and ESV in Anhui Province. Strong correlations are primarily concentrated in the mining areas of the Huainan-Huaibei mining region and the plains along the river, while the local correlations in the rest of the surrounding areas are mainly L-L and non-significant. The H-H grid areas and L-H grid areas represent the smallest proportion of the total number of grids, accounting for 1.18% and 4.54% of the total number of grids, respectively, and are mainly along the Yangtze River for centralized and continuous development. The main reason is that this region has the Yangtze River, a natural water transportation hub, frequent economic activities, and large carbon emissions. Water bodies are ecologically important and capable of producing high ESV. The L-L grids area has the largest proportion of grids, accounting for 32.53% of the total number of grids, and is mainly distributed around the main urban areas of Huainan City, Huaibei City, and Hefei City. The main reason is that this area is located in the Huaihe River Plain, with gentle terrain dominated by cropland, low carbon emissions, and low vegetation cover, which contributes less to ESV. The number of grids in the H-L agglomeration area ranks second after the L-L agglomeration area, comprising 10.56% of the total grids. These grids are primarily situated in the main urban areas of Huainan, Huaibei, and Maanshan City, transitioning from decentralized to centralized agglomerations.

Discussion

The Relationship between Land Use, Carbon Emissions, and ESV

Existing studies primarily concentrate on administrative boundaries like national, provincial, and municipal levels [32–35], respectively studying

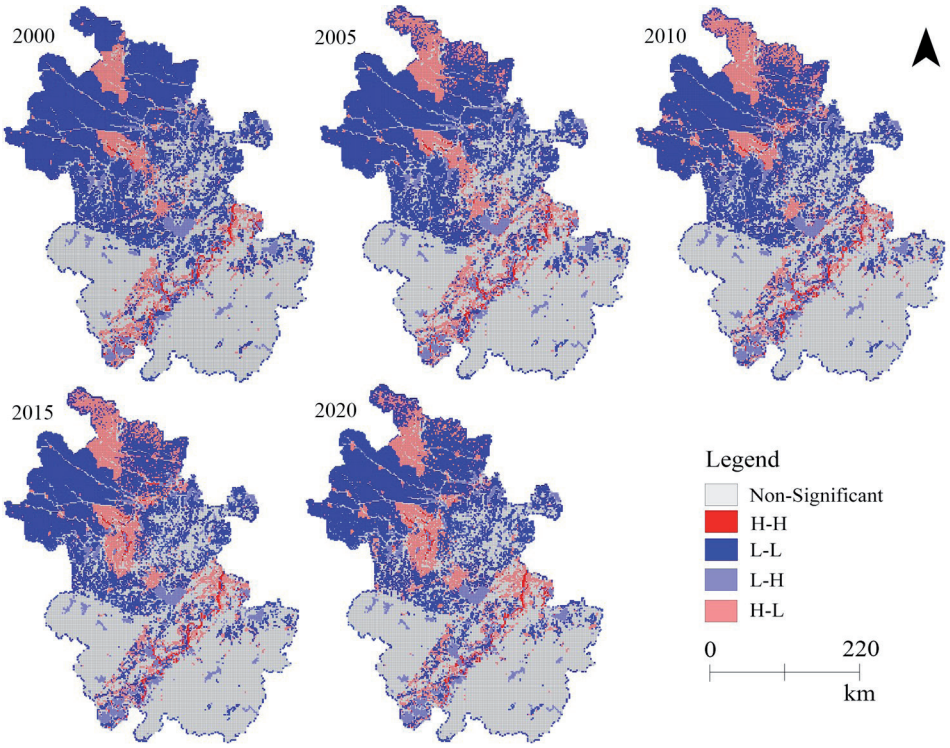

Fig. 6. Bivariate local indicators of spatial association (LISA) cluster graph.

the influence of land use changes on ESV or carbon emissions. However, there's a lack of investigation into the spatial correlation between carbon emissions and ESV. The primary focus of this paper was to examine the spatial correlation and aggregation relationship between carbon emissions and ESV changes resulting from land use alterations in Anhui Province from 2000 to 2020 at the grid scale.

The change in land use mainly includes the change of utilization mode, the change of spatial pattern, and the change of management mode. Land use change affects the function, structure, and ecological process of the ecosystem by changing land type, vegetation cover, and resource distribution, and affects ESV [36]. In addition, land use change also has an impact on regional net carbon emissions by affecting the carbon source/sink structure and carbon cycle system [37].

During 2000-2020, LUCE in Anhui Province showed an obvious upward trend, increasing by $9{,}949.44\times10^4$ tons, with a growth rate of 357.05%. Construction land is the main source of LUCE. From 2000 to 2020, driven by the "integration" strategy of the Yangtze River Delta city cluster, Anhui Province's urbanization level has increased rapidly, and the area of construction land and energy consumption has increased significantly, resulting in a significant increase in carbon emissions of construction land [38, 39]. In addition, the expansion of construction land in Anhui Province is non-linear with the increase of LUCE. Construction land in Anhui Province has always maintained expansion, and its proportion in the province has increased from 6.05% to 9.42%. However, LUCE showed a small decline in the 2015-2020 period, decreasing by 278.85×10^4 tons, indicating that the increase in carbon emissions cannot be attributed to the expansion of construction land alone and that factors such as urbanization level and energy use efficiency also have a significant impact on carbon emission levels [40, 41].

ESV in Anhui Province shows an M-shaped growth trend between 2000 and 2020, with a slight increase of 1.14%. Despite the decline in cropland and grassland areas and the notable expansion of construction land, ESV continues to grow. This resilience is attributed to the high ecological service value of forestland and water [42]. In addition, the regional difference of the ESV supply-demand relationship in Anhui Province is obvious, and the ESV intensity in southern Anhui Province is higher than that in northern Anhui Province. Niu Junjun et al. believe that the differences in resource distribution and topographic characteristics of Anhui Province are the main reasons for this phenomenon [42]. Anqing, Huangshan, and Xuancheng in southern Anhui Province are mountainous, the expansion of construction land is not obvious, and the land use type is dominated by forestland and water, which play an important ecological regulatory role and provide 85%-94% of the ESV in Anhui Province [43]. In contrast, coal mining in the northern part of Anhui Province, particularly in the mining areas of Huainan and Huaibei, has resulted in surface subsidence and water accumulation [44]. This has led to an expansion of water bodies, a reduction in cropland area, and an overall increase in ESV.

An evident negative spatial correlation between carbon emission intensity and ESV intensity is observed in Anhui Province, with distinct clustering evident around the Huainan-Huibei mining area and cities along the river, including Wuhu, Tongling, and Maanshan. Similar to the spatial relation obtained by [45], take Chengdu-Chongqing urban agglomeration in China as the research object. The local spatial aggregation characteristics of the two are similar to the results of [46] research, which shows the development trend of dispersed to centralized. The province has developed coal industry chain clusters, primarily located in Huainan and Huaibei, aiming to enhance regional core competitiveness and achieve rapid economic development through the synergy of industry clusters [47]. In central Anhui Province, cities such as Maanshan, Wuhu, and Tongling have accelerated the process of new urbanization and industrialization through large-scale undertaking of industries in coastal cities and realized intensive urban development.

LUCE Prediction

The forecasting of carbon emissions in this paper employs the GM (1, 1) gray model alongside the PLUS land use prediction model. Additionally, employing the gray model directly for predicting carbon emissions from construction land helps prevent errors stemming from multiple predictions with IPCC energy conversion factors [10].

The forecast results show that LUCE in Anhui Province is in a state of constant growth and eventually stabilization, but it is difficult to achieve carbon emissions before 2030 (Fig. 7). Lu Yanfei et al. believe that Anhui Province is expected to achieve the carbon peak before 2040 under the condition of maintaining the historical development status [48]. However, the growth rate of LUCE in Anhui Province from 2020 to 2030 is significantly lower than that from 2010 to 2020. LUCE in Anhui Province increased from 12735.98×10^4 tons in 2020 to 15630.62×10^4 tons in 2030, with a total increase of 2894.64×10^4 tons, an average annual increase of 2.27%. The decrease in the external expansion rate of construction land is an important reason for the slowing down of the growth rate of LUCE. Since Anhui Province fully joined the Yangtze River Delta city cluster in 2019, intensive land management has been further strengthened [49, 50]. In the forecast results of this paper, construction land in Anhui Province will expand by 1371.80 km^2 from 2020 to 2030, with an average annual growth rate of 1.04%, significantly lower than the 2.69% from 2010 to 2020.

LUCE trend in Anhui Province's prefecture-level cities from 2000 to 2030, indicating a general upward trajectory (Fig. 8). Industrial resource-based cities such as Huaibei City, Maanshan City, Huainan City, and Anqing City are the main carbon sources, accounting for 60.72%-71.98% of the net carbon emissions in Anhui Province. Consequently, regulating carbon emissions in resource cities becomes pivotal for achieving the dual-carbon target. The data reveals a varied slowdown in the growth rate of carbon emissions from resource cities between 2020 and 2030. Notably, Huainan and Maanshan cities exhibit the most significant reductions, with average annual carbon emissions growth rates declining to 2.66% and 0.85%, respectively.

The research indicates that by 2030, construction land, forestland, and water areas in Anhui Province will cover 10.41%, 25.58%, and 4.96% of the total area, respectively. Net carbon emissions are projected to rise,

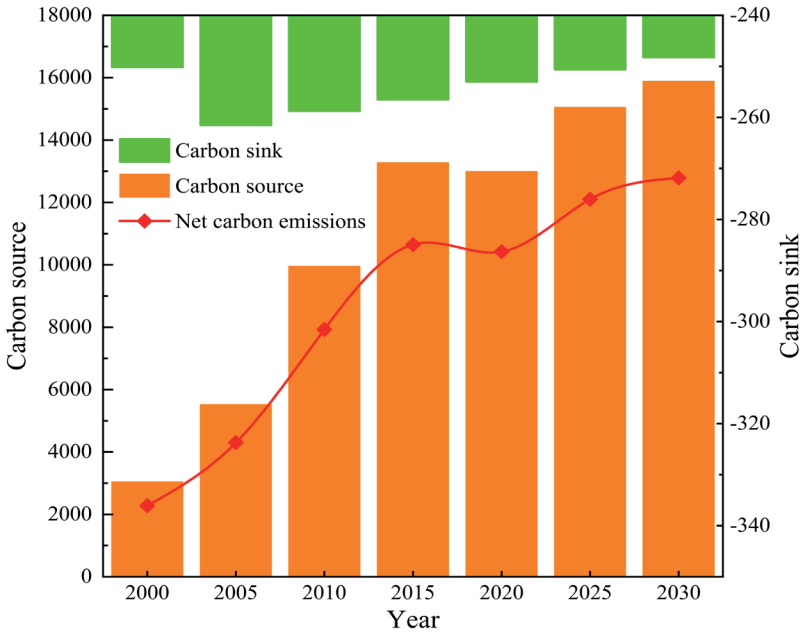

Fig. 7. Carbon source/sink from land use change (10^4 t).

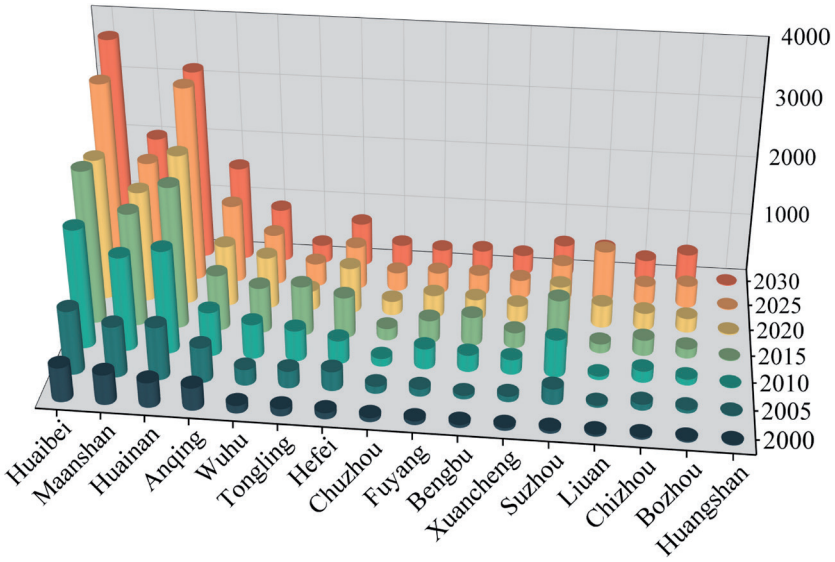

Fig. 8. Carbon emissions by prefecture-level city (10^4t).

far exceeding carbon sinks. Meeting the target of peak carbon dioxide emissions by 2030 continues to pose a significant challenge. Regarding carbon emission spatial patterns, industrial resource-centric cities like Huaibei, Maanshan, Huainan, and Anqing emerge as primary carbon sources, contributing 60.72% to 71.98% of the province's total emissions.

This paper proposes the following recommendations for the urban development traits in Anhui Province: (1) To address the challenges posed by major carbon-emitting cities like Huainan, Huaibei, and Maanshan, predominantly industrial hubs, efforts should be directed towards restraining the expansion of construction land, optimizing land resource utilization, prioritizing the shift of resource cities towards eco-friendly industries, addressing historical resource depletion, and strategically enhancing water bodies and forest cover to bolster carbon sequestration. These measures aim to sustain economic growth, mitigate carbon emissions, enhance ESV, and advance high-quality regional development and the dual-carbon objective. (2) For low-carbon cities such as Huangshan, Bozhou, and Lu'an, where cultural tourism is the mainstay, we should continue to strengthen the protection of forestland and water areas, construct reasonable ecosystems, improve eco-efficiency, optimize the distribution of resources, and increase the ESV of the region so that we can better act as a guarantee of ecological security.

Prospect and Deficiency

The study has the following limitations: (1) The standardization of carbon emission coefficients across various land types, both domestically and internationally, remains incomplete. This paper draws on the research results of the IPCC and related scholars and combines large-scale statistical data at the provincial level to estimate the carbon emission coefficients, but due to the different realities, these results may have a certain degree of spatial heterogeneity. Future research should delve into the carbon emissions produced by various land use types in cities with diverse dominant industries and tailor carbon emission coefficients to suit each city's characteristics. (2) When predicting future carbon emissions from construction land, this study encountered limitations in acquiring energy data. Only 10 types of energy data were selected for carbon emission accounting, overlooking policy regulations' binding nature, such as carbon emission reduction. Therefore, more comprehensive models and methods can be selected in the future to take local policies such as carbon emission reduction into account.

Conclusions

(1) Various levels of transformation were observed among land types in Anhui Province from 2000 to 2020, totaling 11,374.77km^2 in transferred area, constituting 8.12% of the study area's total. Cropland and construction land are the main land types that undergo transfer changes, in which construction land area increases by 4726.91km^2, and cropland contributes the most to the construction land area, accounting for about 98.34%.

(2) From 2000 to 2020, the net carbon emissions displayed an inverted "V" growth pattern, marked by nodes in 2010 and 2015. Initially, carbon emissions surged between 2000 and 2010, followed by a deceleration from 2010 to 2015, and subsequently a decline from 2015 to 2020. The carbon emission intensity was on the rise, with an overall spatial distribution increasingly concentrated. The core, centered around the Huainan-Huaibei mining area in

the northern part of Anhui Province, exhibits a double-core circular distribution. Conversely, the southern part, aligned with the Yangtze River, demonstrates a belt-shaped aggregation, extending from east to south.

(3) From 2000 to 2020, the ESV in Anhui Province followed an M-shaped growth trajectory, with 2010 marking the trough point. Over this period, ESV experienced an overall increase of CNY 28.89×10^8, representing a growth rate of 1.14%. ESV intensity in Anhui Province differs significantly from north to south, and the ESV intensity in the south of Anhui Province is higher than that in the north. The ESV intensity grid in southern Anhui Province is dominated by levels IV and V, with a large ESV contribution rate, and is an important ecological regulation base in Anhui Province.

(4) In Anhui Province, there exists a notable adverse spatial correlation between the intensity of ESV and the intensity of LUCE. As carbon emissions rise, ESV diminishes accordingly. Spatially, these exhibit evident aggregation patterns, with high-concentration zones primarily situated within urban areas along the riverside city belt and insignificant aggregation in the surrounding areas. Additionally, H-L aggregation areas cluster around the Huainan and Huaibei mining areas, while L-L aggregation areas are dispersedly located around H-L clusters.

(5) From 2020 to 2030, there was a staged growth trend in net carbon emissions in Anhui Province, rising by $2{,}894.64\times10^4$ tons. The primary carbon sources are the industrial resource-oriented cities of Huaibei, Maanshan, Huainan, and Anqing, contributing 60.72% to 71.98% of the total CE in the province.

Acknowledgments

This research is supported by Natural Science Research Project of Anhui Educational Committee (2023AH051208), Open Foundation of State Key Laboratory of Mining Response and Disaster Prevention (SKLMRDPC21KF19), the Scientific Research Foundation for High-level Talents of Anhui University of Science and Technology (2023yjrc43) and Open Foundation of Anhui Green Mine Engineering Research and Development Center. The authors wish to thank Huaibei Mining (Group Co.), Ltd. for comprehensive technical support.

Conflict of Interest

The authors declare no conflict of interest.

References

1. LIU L., GU J., MARASENI T.N., NIU Y., ZENG J., ZHANG L., XU L. Household CO_2 Emissions: Current Status and Future Perspectives. International Journal of Environmental Research and Public Health, **17** (19), 7077, **2020**.
2. MEI H., LI Y.P., SUO C., MA Y., LV J. Analyzing the impact of climate change on energy-economy-carbon nexus T system in China. Applied Energy, **262**, 114568, **2020**.
3. QIAN L., YI H., SHEN M., WANG M. Coupling coordination and spatio-temporal evolution of land-use benefits under the dual carbon goal: A case study in Anhui, China. Science of The Total Environment, **903**, 166123, **2023**.
4. LI J., JIAO L., LI F., LU X., HOU J., LI R., CAI D. Spatial disequilibrium and influencing factors of carbon emission intensity of construction land in China. Journal of Cleaner Production, **396**, 136464, **2023**.
5. CEHN W., GU T., FANG C., ZENG J. Global urban low-carbon transitions: Multiscale relationship between urban land and carbon emissions. Environmental Impact Assessment Review, **100**, 107076, **2023**.
6. ZHOU Y., CHEN M., TANG Z., MEI Z. Urbanization, land use change, and carbon emissions: Quantitative assessments for city-level carbon emissions in Beijing-Tianjin-Hebei region. Sustainable Cities and Society, **66**, 102701, **2021**.
7. HE Q., TAN S., XIE P., LIU Y., LI J. Re-assessing Vegetation Carbon Storage and Emissions from Land Use Change in China Using Surface Area. Chin. Chinese Geographical Science, **29**, 601, **2019**.
8. ZORROLLA-MIRAS P., PALOMO I., GOMEZ-BAGGETHUN E., MARTIN-LOPEZ B., LOMAS P.L., MONTES C. Effects of land-use change on wetland ecosystem services: A case study in the Doñana marshes (SW Spain). Landscape and Urban Planning, **122**, 160, **2014**.
9. LI X., HU S., JIANG L., HAN B., LI J., WEI X. Spatiotemporal Patterns and the Development Path of Land-Use Carbon Emissions from a Low-Carbon Perspective: A Case Study of Guizhou Province. Land, **12**, 1875, **2023**.
10. WEI B., KASIMU A., REHEMAN R., ZHANG X., ZHAO Y., AIZIZI Y., LIANG H. Spatiotemporal characteristics and prediction of carbon emissions/absorption from land use change in the urban agglomeration on the northern slope of the Tianshan Mountains. Ecological Indicators, **151**, 110329, **2023**.
11. LUO X., AO X., ZHANG Z., WAN Q., LIU X. Spatiotemporal variations of cultivated land use efficiency in the Yangtze River Economic Belt based on carbon emission constraints. Journal of Geographical Sciences, **30**, 535, **2020**.
12. XU Y., SUN L., WANG B., DING S., GE X., CAI S. Research on the Impact of Carbon Emissions and Spatial Form of Town Construction Land: A Study of Macheng, China. Land, **12**, 1385, **2023**.
13. CERNUSCA A., BAHN M., BERNINGER F., TAPPEINER U., WOHIFAHRT G. Effects of Land-Use Changes on Sources, Sinks and Fluxes of Carbon in European Mountain Grasslands. Ecosystems, **11**, 1335, **2008**.
14. WANG M., HU Z., WANG X., LI X., WANG Y., LIU H., HAN C., CAI J., ZHAO W. Spatio-Temporal Variation of Carbon Sources and Sinks in the Loess Plateau under Different Climatic Conditions and Land Use Types. Forests, **14**, 1640, **2023**.
15. LI W., XIANG M., DUAN L., LIU Y., YANG X., MEI H., WEI Y., ZHANG J., DENG L. Simulation of land

utilization change and ecosystem service value evolution in Tibetan area of Sichuan Province. Alexandria Engineering Journal, **70**, 13, **2023**.
16. ZHANG Y., HU X., WEI B., ZHANG X., TANG L., CHEN C., WANG Y., YANG X. Spatiotemporal exploration of ecosystem service value, landscape ecological risk, and their interactive relationship in Hunan Province, Central-South China, over the past 30 years. Ecological Indicators, **156**, 111066, **2023**.
17. WEI W., LI Y., MA L., XIE B., HAO R., CHEN D., YANG S. Carbon emission change based on land use in Gansu Province. Environmental Monitoring and Assessment, **196**, 311, **2024.**
18. ZHANG Y., LI J., LIU S., ZHOU J. Spatiotemporal Effects and Optimization Strategies of Land-Use Carbon Emissions at the County Scale: A Case Study of Shaanxi Province, China. Sustainability, **16**, 4104, **2024**.
19. GUO P., ZHANG F., WANG H. The response of ecosystem service value to land use change in the middle and lower Yellow River: A case study of the Henan section. Ecological Indicators, **140**, 109019, **2022**.
20. XU J. Study on spatiotemporal distribution characteristics and driving factors of carbon emission in Anhui Province. Scientific Reports, **13**, 14400, **2023**.
21. ZHANG M., DONG S., LI F., XU S., GUO K., LIU Q. Spatial–Temporal Evolution and Improvement Measures of Embodied Carbon Emissions in Interprovincial Trade for Coal Energy Supply Bases: Case Study of Anhui, China. International Journal of Environmental Research and Public Health, **19**, 17033, **2022**.
22. YANG J., HUANG X. The 30 m annual land cover dataset and its dynamics in China from 1990 to 2019. Earth System Science Data, **13**, 3907, **2021**.
23. ZHANG C., ZHAO L., ZHANG H., CHEN M., FANG R., YAO Y., ZHANG Q., WANG Q. Spatial-temporal characteristics of carbon emissions from land use change in Yellow River Delta region, China. Ecological Indicators, **136**, 108623, **2022**.
24. WANG M., WANG Y., TENG F., JI Y. The spatiotemporal evolution and impact mechanism of energy consumption carbon emissions in China from 2010 to 2020 by integrating multisource remote sensing data. Journal of Environmental Management, **346**, 119054, **2023**.
25. FANG J., GUO Z., PARK S., CHEN A.-P. Terrestrial vegetation carbon sinks in China,1981-2000. Science in China (Series D:Earth Sciences), **9,** 1341, **2007**.
26. XIE G., ZHANG C., ZHEN L., ZHANG L. Dynamic changes in the value of China's ecosystem services. Ecosystem Services, **26**, 146, **2017**.
27. ZHANG Y., HU X., WEI B., ZHANG X., TANG L., CHEN C., WANG Y., YANG X. Spatiotemporal exploration of ecosystem service value, landscape ecological risk, and their interactive relationship in Hunan Province, Central-South China, over the past 30 years. Ecological Indicators, **156**, 111066, **2023**.
28. CUI J., LIU S., ZENG B., XIE N. A novel grey forecasting model and its optimization. Applied Mathematical Modelling, **37**, 4399, **2013**.
29. YONG W., XIE Y., RONG L., HAO Z. Population prediction and resource allocation in megacities from the optimum population perspective: A case study of Beijing, Shanghai, Guangzhou and Shenzhen. Acta Geographica Sinica, **76**, 352, **2021**.
30. LIANG X., GUAN Q., CLARKE K.C., LIU S., WANG B., YAO Y. Understanding the drivers of sustainable land expansion using a patch-generating land use simulation (PLUS) model: A case study in Wuhan, China. Computers, Environment and Urban Systems, **85**, 101569, **2021**.
31. ZHU Y., GAO Y., WANG W., LU N., XU R., LIU B., LI J. Assessment of emission reduction effect in Beijing, Tianjin and surrounding 26 cities from January to March in 2020 during the epidemic of COVID-19. China Environmental Science, **41**, 505, **2021**.
32. LONG Z., ZHANG Z., LIANG S., CHEN X., DING B., WANG B., CHEN Y., SUN Y., LI S., YANG T. Spatially explicit carbon emissions at the county scale. Resources, Conservation and Recycling, **173**, 105706, **2021**.
33. LUO H., GAO X., LIU Z., LIU W., LI Y., MENG X., YANG X., YAN J., SUN L. Real-time Characterization Model of Carbon Emissions Based on Land-use Status: A Case Study of Xi'an City, China. Journal of Cleaner Production, **434**, 140069, **2024**.
34. LUO H., LI Y., GAO X., MENG X., YANG X., YAN J. Carbon emission prediction model of prefecture-level administrative region: A land-use-based case study of Xi'an city, China. Applied Energy, **348**, 121488, **2023**.
35. XIA C., DONG Z., WU P., DONG F., FANG K., LI Q., LI X., SHAO Z., YU Z. How urban land-use intensity affected CO_2 emissions at the county level: Influence and prediction. Ecological Indicators, **145**, 109601, **2022**.
36. JING X., TIAN G., HE Y., WANG M. Spatial and temporal differentiation and coupling analysis of land use change and ecosystem service value in Jiangsu Province. Ecological Indicators, **163**, 112076, **2024**.
37. LUO Y., LI X., CHEN L., ZHANG H., WANG M., CHEN W. Low carbon development patterns of land use under complex terrain conditions: The case of Chongqing in China. Ecological Indicators, **155**, 110990, **2023**.
38. CHANG Q., SHA Y., CHEN Y. The Coupling Coordination and Influencing Factors of Urbanization and Ecological Resilience in the Yangtze River Delta Urban Agglomeration, China. Land, **13**, 111, **2024**.
39. XU Z., YIN Y. Regional Development Quality of Yangtze River Delta: From the Perspective of Urban Population Agglomeration and Ecological Efficiency Coordination. Sustainability, **13**, 12818, **2021**.
40. LOU T., MA J., LIU Y., YU L., GUO Z., HE Y. A Heterogeneity Study of Carbon Emissions Driving Factors in Beijing-Tianjin-Hebei Region, China, Based on PGTWR Model. International Journal of Environmental Research and Public Health, **19**, 6644, **2022**.
41. ZHANG D., WANG Z., LI S., ZHANG H. Impact of Land Urbanization on Carbon Emissions in Urban Agglomerations of the Middle Reaches of the Yangtze River. International Journal of Environmental Research and Public Health, **18**, 1403, **2021**.
42. NIU J., MAO C., XIANG J. Based on ecological footprint and ecosystem service value, research on ecological compensation in Anhui Province, China. Ecological Indicators, **158**, 111341, **2024**.
43. HU S., CHRN L., LI L., ZHANG T., YUAN L., CHENG L., WANG J., WEN M. Simulation of Land Use Change and Ecosystem Service Value Dynamics under Ecological Constraints in Anhui Province, China. International Journal of Environmental Research and Public Health, **17**, 4228, **2020**.
44. XIAO W., HU Z., LI J., ZHANG H., HU J. A study of land reclamation and ecological restoration in a resource-exhausted city – a case study of Huaibei in China. International Journal of Mining, Reclamation and Environment, **25**, 332, **2011**.

45. 45. CHEN Y., LU H., LI J., XIA J. Effects of land use cover change on carbon emissions and ecosystem services in Chengyu urban agglomeration, China. Stochastic Environmental Research and Risk Assessment, **34**, 1197, **2020**.
46. ZHANG R., YU K., LUO P. Spatio-Temporal Relationship between Land Use Carbon Emissions and Ecosystem Service Value in Guanzhong, China. Land, **13**, 118, **2024**.
47. ZHANG M., DONG S., LI F., XU S., GUO K., LIU Q. Spatial–Temporal Evolution and Improvement Measures of Embodied Carbon Emissions in Interprovincial Trade for Coal Energy Supply Bases: Case Study of Anhui, China. International Journal of Environmental Research and Public Health, **19**, 17033, **2022**.
48. LU Y., XUAN W., ZHAO L. Spatio-temporal Evolution of Carbon Emissions and Prediction of Carbon Peak Path in Anhui Province: Based on Extended STIRPAT Model and Ridge Regression Model. Areal Research and Development, **43**, 146, **2024**.
49. ZHANG T., CHEN L., YU Z., ZANG J., LI L. Spatiotemporal Evolution Characteristics of Carbon Emissions from Industrial Land in Anhui Province, China. Land, **11**, 2084, **2022**.
50. GAO Z.-Q., TAO F., WANG Y.-H., ZHOU T. Potential ecological risk assessment of land use structure based on MCCA model: A case study in Yangtze River Delta Region, China. Ecological Indicators, **155**, 110931, **2023**.